EXPERIMENTAL STUDY OF DIELECTRIC DISC ANTENNA BACKED BY A METAL PLATE

By (MRS.) R. CHATTERJEE, Sqn. Ldr. LAKHMIR SINGH* AND S. K. CHATTERJEE

[*Department of Electrical Communication Engineering, Indian Institute of Science, Bangalore-12, India*]

ABSTRACT

Numerical evaluation of some of the theoretical aspects of the earlier theoretical study by the authors on surface waves launched on dielectric discs with a metal disc sandwiched between them is presented. Experimental results on the transverse and radial field decay and vertical and horizontal radiation patterns, when the dielectric discs, are excited at X band by a double cone placed symmetrically on both sides of the structure are reported.

1. INTRODUCTION

The brilliant memoir by Arnold Sommerfeld[1] on a formal solution for a vertical electric dipole in the plane interface between an insulating half-space (air) and a conducting half-space (earth), the monumental paper by the same author[2] extending his earlier analysis, Zenneck's[3] work on the solution of Maxwell's equations which was in the form of a wave supported by a plane interface between homogeneous media, one of which is an insulator, Hermann Weyl's[4] reformulation of the problem of a dipole above a conducting half-space, James Wait's[5] brilliant exposition of surface waves, Barlow and Brown's[6] illuminating discussion on surface waves and work by numerous other authors have made significant contributions to the field of electromagnetic surface waves. In a recent paper the authors[7] have developed the theory of surface waves on a dielectric disc backed by a metal plate. The object of the paper is to present solutions of characteristic equations as function of dielectric disc thickness(a) and dielectric constant (ϵ_r), numerical evaluation of a delay ratio as $f(a, \epsilon_r)$, experimental results on transverse and radial field decay and radiation patterns in the horizontal and vertical planes and attenuation constants in the transverse and radial directions when two dielectric discs with a metal-disc sandwiched between them is excited at X band.

---

*Sqn. Ldr. Lakhmir Singh is at present at the Air Headquarters, New Delhi.

2.   CHARACTERISTIC EQUATION

The characteristic equation (see Fig. 1) is[7]
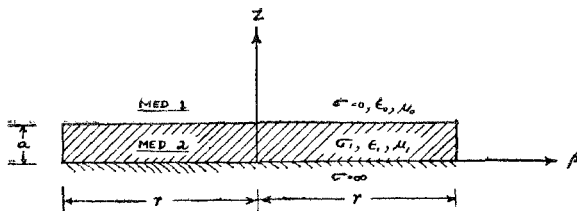
FIG. 1

Coordinate System $(\rho,\, z,\, \phi)$ for the Dielectric Disc backed by metal plate structure

$$\frac{A\,[u_1/(\sigma_1 + j\,\omega\,\epsilon_1)]\,H_1^{(2)}\,(-j\,\gamma\,\rho)\,\sin u_1 a}{A\,H_1^{(2)}\,(-j\,\gamma\,\rho)\,\cos u_1 a}$$

$$= \frac{A\,[u_2/(j\,\omega\,\epsilon_0)]\exp\,(-u_2 a)\,H_1^{(2)}\,(-j\,\gamma\,\rho)}{A\,\exp\,(-u_2 a)\,H_1^{(2)}\,(-j\,\gamma\,\rho)} \tag{1}$$

which yields

$$-u_2 = (\epsilon_r)^{-1}\,u_1 \tan\,(u_1 a) \tag{2}$$

where,

$$u_2^2 = -\gamma^2 - k_2^2$$

$$k_2^2 = \omega^2\,\mu_0\,\epsilon_0$$

$$u_1 = a_1 + j\,b_1$$

$$u_2 = a_2 - j\,b_2$$

$$\gamma = \alpha + j\,\beta$$

$$u_2^2 - u_1^2 = \omega^2\,\mu_0\,\epsilon_0\,(\epsilon_r - 1)$$

$$\epsilon_r = \epsilon_1/\epsilon_0$$

$$k_1^2 = \omega^2\,\mu_1\,\epsilon_1 = -\,(\gamma^2 + u_1^2) \tag{3}$$

a = thickness of each dielectric disc

γ = radial propagation contant

The above equation [2] is solved by plotting $(\epsilon_r)^{-1}\,u_1 \tan u_1\,a$ vs. u_1 as $f(a,\,\epsilon_r)$ and $[u_1^2 + (\omega^2/c^2)\,(\epsilon_r - 1)]^{1/2}$ vs. u_1 as $f(a,\,\epsilon_r)$. The values of u_1 satisfying the equation for different values of ϵ_r and a are obtained from the intersections of the two sets of curves.

3. SOLUTION OF THE CHARACTERISTIC EQUATION

Equation 2 is solved for $\epsilon_r = 1.5$, 2.56, 5.7, 10 and $a = 2$, 4, 6, 8, 10, 15 mm. The left hand side (f_2) vs. u_1 represents a circle of radius $\sqrt{(k_1^2 - k_2^2)}$. The right hand side represented by f_1 is plotted vs. u_1 in the same diagram as f_2. The intersection of the curves f_1 and f_2 for each combination of ϵ_r and a gives the desired values of u_1. The graphical solution for only the case $\epsilon_r = 2.56$, $a = 2mm$ to $a = 15mm$ and $\lambda_0 = 3.14$ cm is shown in Fig. 2. The other sets of curves for different values of ϵ_r are similarly constructed.

4. PERCENTAGE REDUCTION IN PHASE VELOCITY

The values of γ and u_2 are found from the corresponding values of u_1 by using the relations.

$$u_2^2 - u_1^2 = k_2^2 (\epsilon_r - 1) ; \quad u_2^2 = -\gamma^2 - k_2^2 \quad [4]$$

The values of β as $f(a, \epsilon_r)$ are determined from the values of γ assuming α to be small. The phase velocity $v_p (= \omega/\beta)$ of the surface waves and hence the percentage reduction $(c - v_p)/c\%$ in phase velocity as $f(\epsilon_r, a)$ are determined. The results of the computation are presented in Fig. 3. The phase velocity can also be calculated from the rigorous relation.

$$v_p = \frac{\omega}{a_2 b_2} \left[\frac{-(a_2^2 - b_2^2 + k_2^2) \pm \sqrt{[(a_2^2 - b_2^2 + k_2^2)^2 + 4 a_2^2 b_2^2]}}{2} \right]^{1/2} \quad [5]$$

where,

$$a_1 = \left[\frac{-[(\omega^2/c^2) \epsilon_r + \alpha^2 - \beta^2] \pm \sqrt{\{[(\omega^2/c^2) \epsilon_r + \alpha^2 - \beta^2]^2 + 4 \alpha^2 \beta^2\}}}{2} \right]^{1/2} \quad [6]$$

$$a_2 = \left[\frac{\{(\omega^2/c^2)(\epsilon_r - 1) + a_1^2 - b_1^2\} \pm \{[(\omega^2/c^2)(\epsilon_r - 1) + (a_1^2 - b_1^2)]^2 + 4 \alpha^2 \beta^2\}}{2} \right]^{1/2} \quad [7]$$

$$b_1 = -(\alpha\beta)/a_1 ; \quad b_2 = (\alpha\beta)/a_2 \quad [8]$$

5. DIELECTRIC DISC ANTENNA

Fig. 4 shows a photograph of the antenna with its launching device at X band. Fig. 5 shows the dimensional sketch of the antenna and launcher. The disc assembly consists of two dielectric discs of equal diameter (18 inches) and thickness $a = 4 mm$ sandwiching an aluminium disc of the same diameter. The function of the launching cone is to convert energy from the coaxial mode (TEM) to a radially propagating E_0 mode surface wave on the
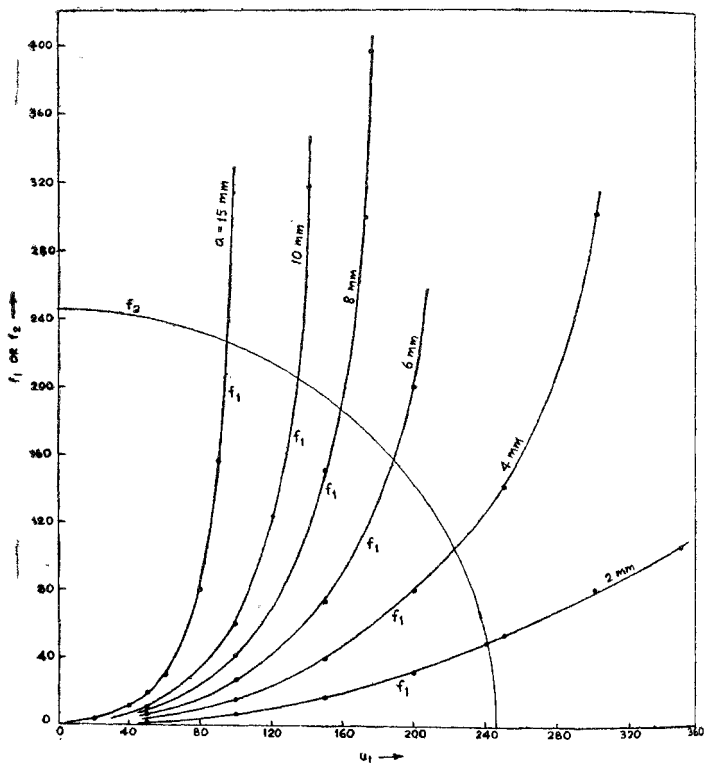
FIG. 2

Solution of eqn. 3–(2) for $\epsilon_r = 2.56$ and $\lambda = 3.14$ cm.
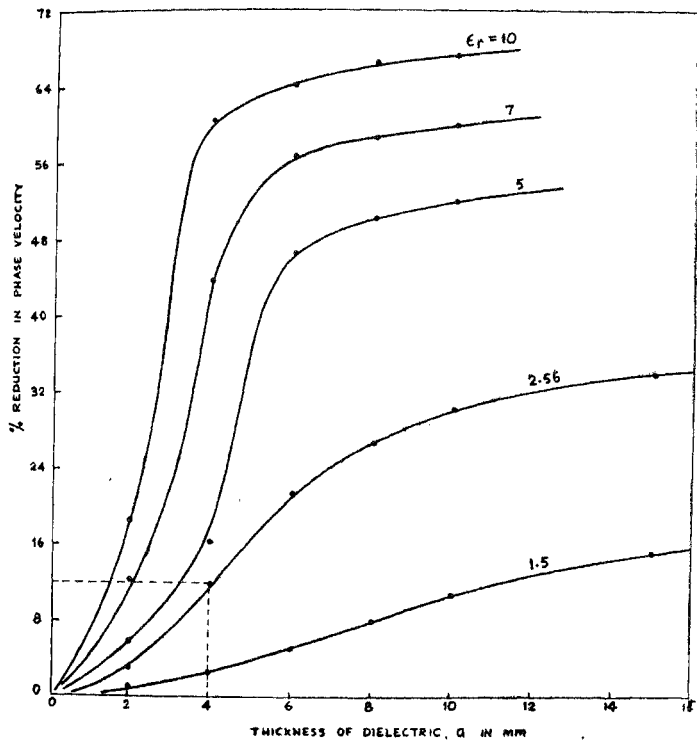
FIG. 3

Percentage reduction in phase velocity as $f(\epsilon_r, a)$ at $\lambda = 3.14$ cm.
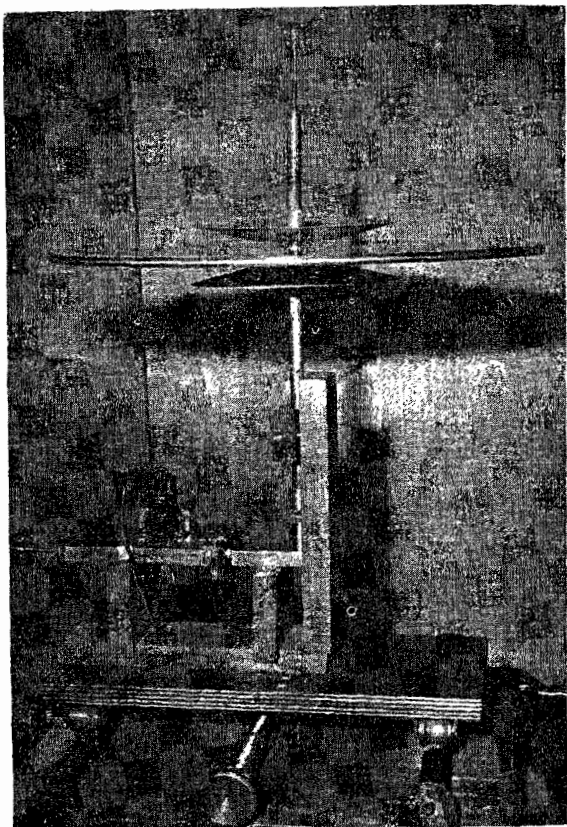
FIG. 4
Photograph of the Dielectric Disc Antenna
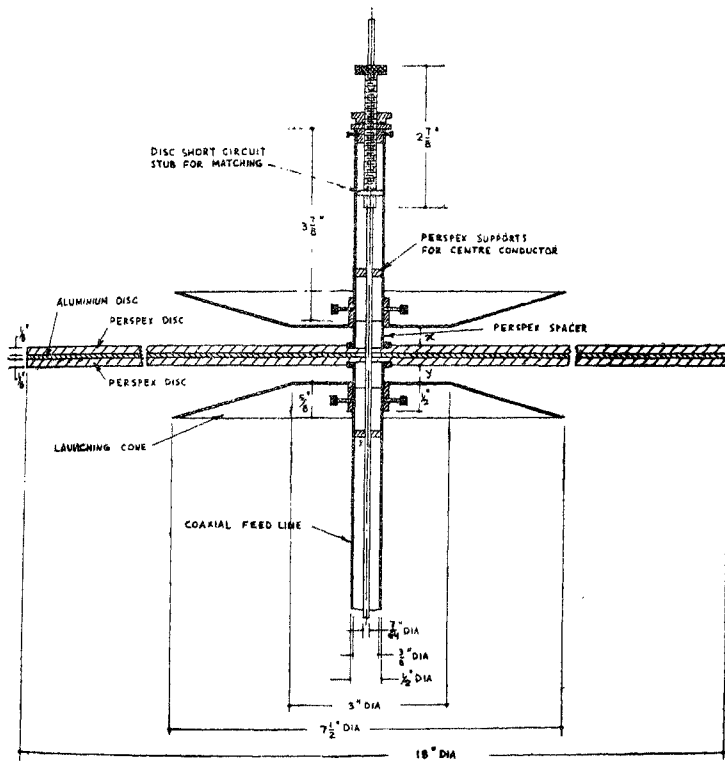
FIG. 5

Sketch of the assembled antenna

dielectric disc. The shape and dimensions of the launching cones are chosen to create conditions favourable for launching the proper mode. The flare angle of the cone is 15 degrees. The flare angle was made small so that surface wave could develop gradually. The design of the flare angle was based on the consideration of not only high launching efficiency but also of the availability of sufficient power convenient for measurement. Provision has been made to vary the distance between the two launching cones and the surface of the dielectric disc assembly. The top and bottom cones can be adjusted independently of each other. The cones are supported on the outer conductor of the rigid coaxial line which is connected to the broad face of a $H_{01}^{\square}$ guide by means of a rectangular to coaxial adapter. The mode transducer consisting of the rectangular guide—rigid coaxial line—cone performs the mode conversion $H_{01}^{\square} \rightarrow T^{\odot} \rightarrow E_0$. The whole antenna assembly is mounted on suitable turntable which has the provision for linear as well as 360 degree rotation arrangement.

6.   FIELD MEASUREMENT

The field distributions on and near the surface of the dielectric disc as $f(z, \rho)$ and for different distances x and y of the launching cone from the dielectric surface were measured with the help of a half wave dipole and a monopole probe. Fig. 6 shows the field distributions E_z in the direction z transverse to the surface of the disc and for different values of ρ, x and y.

7.   GUIDE WAVELENGTH AND PERCENTAGE REDUCTION IN PHASE VELOCITY

Values of guide wavelength λ_g is determined from E_z vs. ρ plot for different launching conditions. Fig. 7 is a typical plot of E_z vs. ρ. The corresponding percentage reduction in phase velocity is calculated from the corresponding values of λ_g and the results are given in Table I.

TABLE 1

λ_g, $(c-v_p)/c\%$, and α_z (db/cm)

x (mm)	y (mm)	h (mm)	(cm)	$(c-v)/c\%$	$\alpha_z db/(cm)$
4	2	0.5	2.84	9.55	55
4	2	5	2 90	7.65	62
4	2	10	2.90	7.65	62
8	2	0.5	2.83	10.3	53
8	2	5	2.86	8.93	54
8	2	10	3.12	0.64	173
16	2	0.5	2.88	8.27	58
16	2	5	2.94	6.38	67
16	2	10	3.10	1.32	124
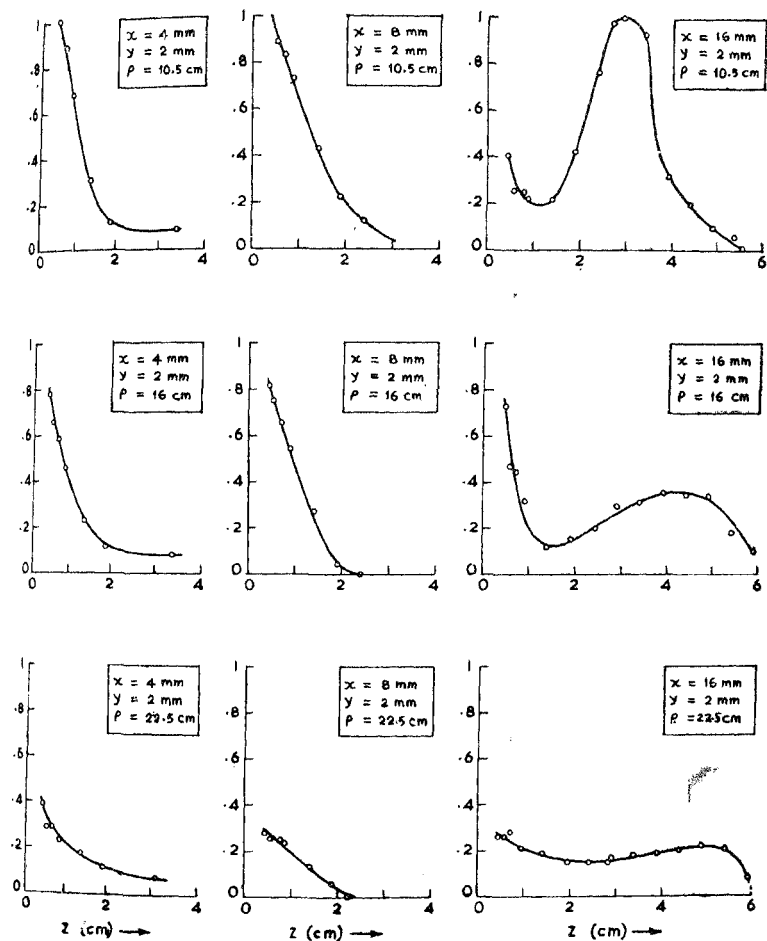
FIG. 6

Observed variation of E_z with z for a 15° cone with different launching conditions
$\rho = 10.5$ cm, 16 cm and 22.5 cm at 3.14 cm wavelength
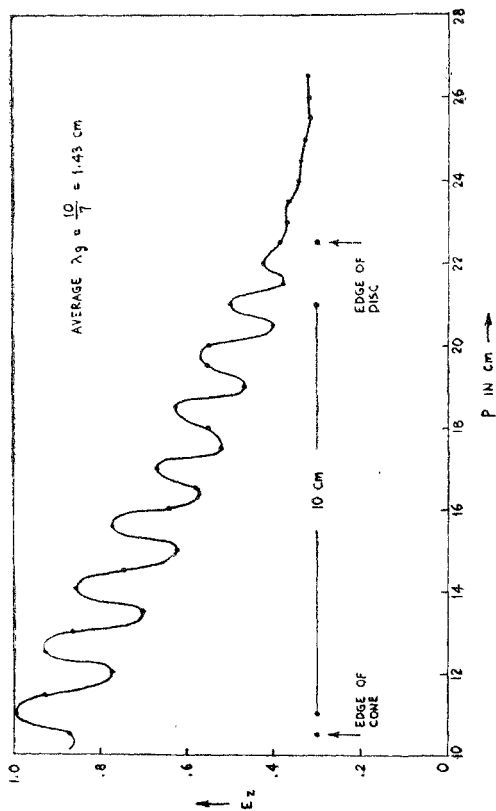
Fig. 7

Calculations of experimental λ_g.

8. DELAY RATIO

The delay ratio $c/v_p = \beta/k_2$ as $f(\epsilon_r, a)$ has been calculated and the results are reported in FIG. 8.

9. ATTENUATION CONSTANT

The attenuation constant in the transverse direction has been computed from the experimental values of λ_g by means of the relation.

$$\alpha_2 = \frac{2\pi}{\lambda_0 \sqrt{(\lambda_0/\lambda_g - 1)}} \text{ nepers/meter} \qquad [9]$$

The results for different launching conditions and height of the probe from the disc surface are given in Table 1. The attenuation constant α_p in the radial direction for the same launching conditions as above and height of the probe has also been calculated from *v.s.w.r.* measurement and using the relation.

$$\alpha_p = (1/l) \tanh^{-1}[1/v.s.w.r.] \text{ nepers/meter} \qquad [10]$$

where, l is the length in metre of the surface waveguide. The result for different launching conditions is reported in Table 2.

TABLE 2

Attenuation constant α_p

x (mm)	y (mm)	h (mm)	v s.w.r.	α_p (db/cm)
4	2	0.5	1.45	0.61
4	2	5	1.39	0.65
4	2	10	1.30	0.74
8	2	0.5	1.63	0.51
8	2	5	2.0	0.40
8	2	10	1.1	1.1
16	2	0.5	2.2	0.35
16	2	5	2.2	0.35
16	2	10	1.5	0.58
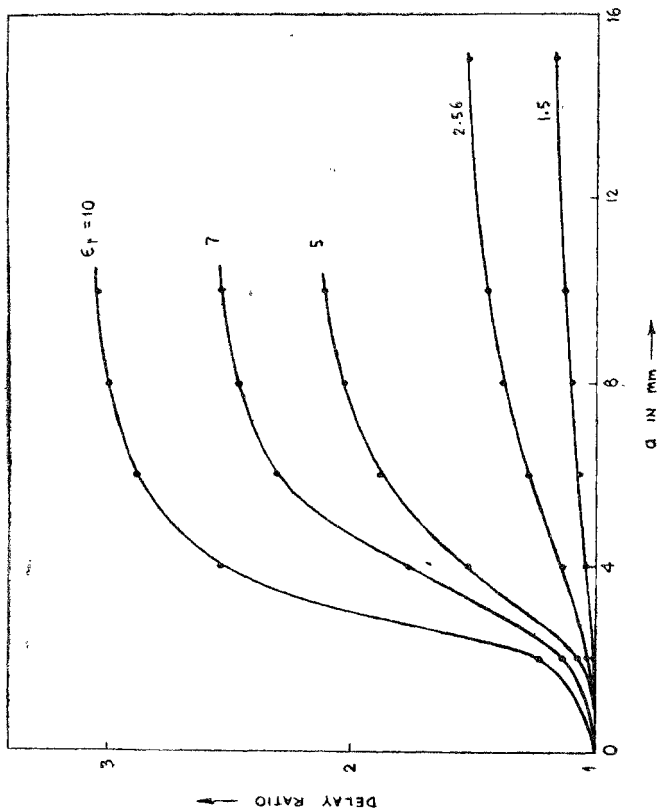
FIG. 8

Variation of delay ratio with dielectric constant and thickness of disc.

The attenuation constants can also be calculated from the rigorous relation.

$$| \alpha | \cong \frac{\sigma_1 \int\limits_{z=0}^{a} \int\limits_{\phi=0}^{2\pi} E^2 r \, d\phi \, dz}{\left(\left| \int\limits_{z=0}^{a} \int\limits_{\phi=0}^{2\pi} E_{z_1} H_{\phi_1}^* r \, d\phi \, dz + \int\limits_{z=a}^{\infty} \int\limits_{\phi=0}^{2\pi} E_{z_2} H_{\phi_2}^* r \, d\phi \, dz \right| \right)} \tag{12}$$

which reduces to

$$| \alpha | = [(A^2 + B^2)/(C^2 + D^2)]^{1/2} \tag{13}$$

for small argument approximations of the cylinder functions involved in [12] and

$$| \alpha | = [(E^2 + F^2)/(G^2 + H^2)]^{1/2} \tag{14}$$

for large argument approximations, where A, B, C etc., are functions of a, ϵ_r, ω and σ_1.

10. RADIATION PATTERNS

A large number of horizontal and vertical radiation patterns were taken for different launching conditions. Some typical radiation patterns are shown in Figures 9 and 10.

11. DISCUSSION

(i) It has been observed that the field variations in the radial direction is oscillatory very near the launching cone but tends to almost a constant value a few guide wavelength away from the cone. The oscillatory nature of the field near the cone may be ascribed to the surface wave field being contaminated with source radiation from the cone modified by the presence of the structure. The tendency for the field distribution to attain a value which decreases very slowly in the radial direction due to the dielectric loss in the structure shows that proper surface wave has been launched.

The field distributions in the transverse direction (z) shows a rapid decay for some launching conditions. This shows that proper surface wave can be launched with good efficiency on the structure by a proper adjustment of the launching device.
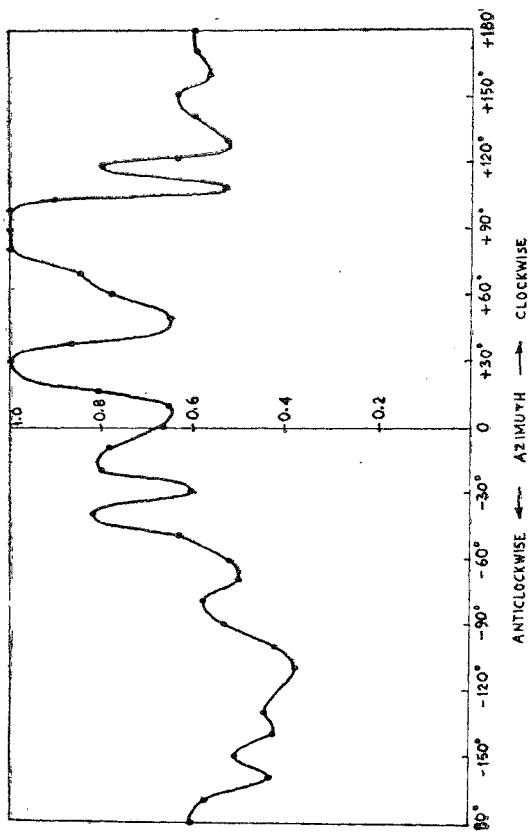
Fig. 9

Observed horizontal radiation pattern at 3.4 cm wavelength.
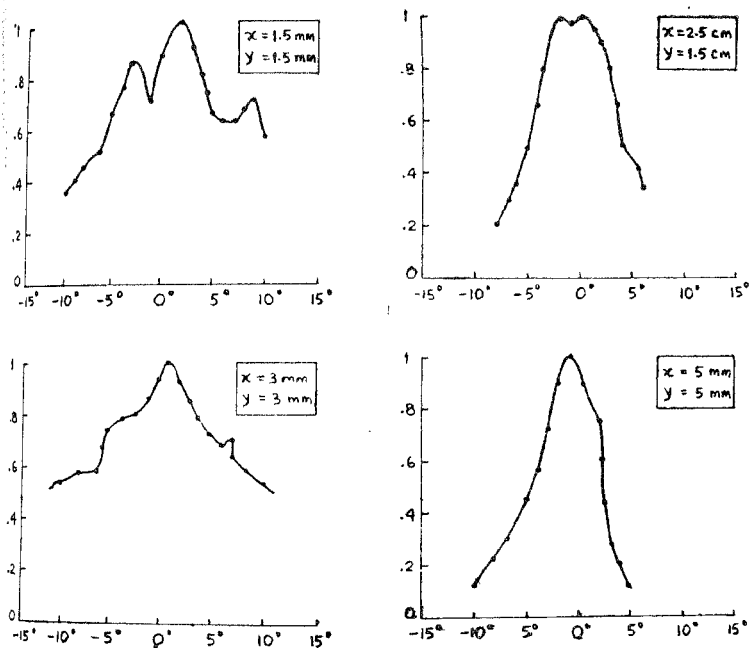
FIG. 10

Observed vertical radiation pattern for *a* 15° cone measured from a distance of 18 feet from the disc with different launching cconditions at 3.14 cm wavelength.

(ii) *Guide wavelength* :   The theoretical value of the guide wavelength is $\lambda_g = 2.763$ cm. derived for the experimental disc having $a = 4\,mm$, $\lambda_g = 3.14$ cm. the percentage variation in phase velocty being 12%. The difference between the theoretical λ_g (theo) and experimental λ_g (expl) under different launching conditions and for different heights of the field measuring probe is given in Table 3.

TABLE 3

λ_g (theo) $\sim \lambda_g$ (expl.)

x (mm)	y (mm)	h (mm)	λ_g (expl.) $\sim \lambda_g$ (theo)
4	2	0.5	0.077
4	2	5	0.137
4	2	10	0.137
8	2	0.5	0.067
8	2	5	0.097
8	2	10	0 357
16	2	0.5	0.117
16	2	5	0 177
16	2	10	0.337

The theoretical value of λ_g is derived for pure surface wave mode. The experimental value is sensitive to launching conditions and also the height at which the field is being measured. The agreement is better for the value measured closer to the surface for all launching conditions. This is probably due to the fact that as the distance in the transverse direction (z) is increased, probably the free space wave field becomes more predominant and experimental λ_g approaches the free space value.

(iii) *Percentage reduction in phase velocity* : The theoretical value of the reduction in phase velocity is 12% corresponding to the experimental disc. But the experimental value closest to the theoretical value is 10.3% which corresponds to the launching condition $x = 8$ *mm* and $y = 2$ *mm* and for $h = 0.5$ *mm*. The theoretical value is derived on the basis of source free condition, whereas, the experimental values depend on the launching conditions. In other words, the theory is derived on the assumption of pure surface wave but in the experiment slight contamination on the surface wave field cannot be overruled, even when the launching efficiency is high.

(iv) *Attenuation constant* : It is observed from Table 1 and 2 that the attenuation constants in the transverse (α_z) and in the radial (α_ρ) directions are sensitive to the launching conditions and also to h. For the same launching conditions $x = 8$ *mm*, $y = 2$ *mm* and $h = 0.5$ *mm*, the values of $\alpha_z = 53$ *db/cm* and $\alpha_\rho = 0.51$ *db/cm*. This shows that the rate of field decay in the transverse direction is much greater than that along the surface of the disc. This leads to the view that the structure can support a radial cylindrical surface wave of the Zenneck type.

(v) *Radiation patterns*: The radiation patterns in both the horizontal and vertical planes depend on the launching conditions. The patterns in the vertical plane show maxima at angle less than 2 degree. This shows that the antenna is suitable for low angle radiation. The pattern in the horizontal plane is expected to have an uniform angular distributions. But the experimental pattern (see Fig. 9) shows maxima and minima. The reason for the divergence from the omnidirectional pattern still remains to be explained.

(vi) *Effect of reflection*: The field components[7]

$$E_{z2} = A\,(\gamma \mid \omega\,\epsilon_0)\,\exp\,(-u_2\,z)\,H_0^{(2)}\,(-j\,\gamma\,\rho)$$

$$E_{\rho2} = A\,(u_2/j\,\omega\,\epsilon_0)\,\exp\,(-u_2 z)\,H_1^{(2)}\,(-j\,\gamma\,\rho) \tag{15}$$

were derived on the assumption that the diameter of the dielectric disc is infinitely large and hence the effect of reflection from the edge of the disc was not taken into account. If, however, the effect of reflection is taken into account, the field components will be modified.

The wave impedance at $\rho = r$ (edge of the disc) is

$$z_1\,(\rho = r) = \frac{E_{z1}}{H_{\phi1}} = \frac{\gamma}{\omega\,\epsilon_1}\cdot\frac{H_0^{(2)}(-j\,\gamma\,r)}{H_1^{(2)}(-j\,\gamma\,r)} \tag{16}$$

The free space impedance is $z_0 = 376.7$ ohms. The reflection coefficient is

$$R_\rho = [(z_1 - z_0)/(z_1 + z_0)]$$

$$= \frac{\dfrac{\gamma}{\omega\,\epsilon_1}\,[H_0^{(2)}\,(-j\,\gamma\,r)] - 376.7\,H_1^{(2)}\,(-j\,\gamma\,r)}{\dfrac{\gamma}{\omega\,\epsilon_1}[H_0^{(2)}\,(-j\,\gamma\,r)] + 376.7\,H_1^{(2)}\,(-j\,\gamma\,r)} \tag{17}$$

The field component is therefore modified to the form

$$E' = E_1 + \mid R_\rho \mid E_1 \tag{18}$$

Further work on dielectric disc antenna will appear elsewhere.

12. Conclusions

(i) Pure radial cylindrical surface wave of the Zenneck type can be launched and supported by a dielectric disc backed by a metal plate, by proper adjustment of the launching conditions.

(ii) The structure can be used as a low angle radiator. This property may find useful applications in radar detection of low angle target.

13. ACKNOWLEDGMENT

One of us L. S. is grateful to Air Headquarters, New Delhi for deputation to study M. E. Degree course in Microwave Engineering.

REFERENCES

1. Sommerfeld, A.   ..   ..   *Annln. Phys.*, 1909, **28**, 665.

2. ————————   ..   ..   *Ibid*, 1926, **81**, 1135.

3. Zenneck, J.   ..   ..   *Ibid*, 1907, **23**, 846.

4. Weyl, H.   ..   ..   *Ibid*, 1919, **60**, 481.

5. Wait, J.   ..   ..   Advances in Radio Research, Vol. I, Academic Press, 1964.

6. Barlow, H. M. and Brown, J.   ..   'Radio Surface Waves' Oxford, Clarendon Press, 1962.

7. Chatterjee, S. K.; (Mrs.) Chatterjee, R. and Lakhmir Singh.   *J. Indian Inst. Sci.*, 1969, 51, 217.